Characterization of the Photoacid Diffusion Length §

Shuhui Kang[1], Vivek M. Prabhu*[1], Wen-li Wu[1], Eric K. Lin[1],
Kwang-Woo Choi[2], Manish Chandhok[2], Todd R. Younkin[2], Wang Yueh[2],

[1]Polymers Division, National Institute of Standards and Technology,
100 Bureau Dr, Gaithersburg, MD 20899
[2]Intel Corporation, 2501 NW 229th Avenue, Hillsboro, OR 97124

ABSTRACT

The photoacid diffusion length is a critical issue for extreme ultraviolet (EUV) lithography because it governs the critical dimension (CD), line-edge-roughness (LER), and line-width-roughness (LWR) of photoresist materials. Laboratory-based experimental methods that complement full lithographic testing would enable a rapid screening of materials and process conditions. This paper provides an approach to characterize the photoacid diffusion length by applying a bilayer stack technique. The method involves quantitative measurements of the deprotection kinetics as well as film thickness at each process step: radiation exposure, post-exposure bake, and development. Analogous to a contrast curve, by comparing the film thickness of the bilayer before and after development, the photoacid diffusion length was deduced in a commercial EUV photoresist and compared to EUV lithography. Further, by combining the experiments with kinetics modeling, the measured photoacid diffusion length was predicted. Lastly, based upon the measured kinetics parameters, a criterion was developed that next-generation resists must meet to achieve a 16 nm photoacid diffusion length. These guidelines are discussed in terms of correlations and contributions from the photoacid and resist properties. In particular, the trapping kinetics of the photoacid provides a route to reduce LER and the CD at low dose.

Key words: photoacid diffusion length, photoresist, kinetics, Fourier transform infrared spectroscopy, poly(dimethylsiloxane)

1. INTRODUCTION

As lithographic features are reduced to below 22 nm, the simultaneous reduction of line-edge-roughness (LER), line-width-roughness (LWR), and dose sensitivity become increasingly challenging[1-4]. Chemically amplified resists (CARs)[5,6] require more control of photoacid diffusion in order to print smaller critical dimensions (CD) with LER and LWR less than 2 nm with extreme ultraviolet (EUV) lithography.[7,8] The photoacid diffusion length remains a critical issue even with the emergence of double exposure and double patterning with immersion lithography[9,10] or novel molecular resists.[11-20] A rapid method to characterize the photoacid diffusion length for new formulations could accelerate resist testing, especially with limited access to advanced EUV lithography facilities.

In this paper, we use a bilayer structure to mimic the lithographic interface between exposed and unexposed regions. The method is improved over previous approaches through a poly(dimethylsiloxane) (PDMS) stamping technique. With this bilayer structure, the photoacid diffusion length may be quantified using common laboratory instruments for any photoresist system including commercial photoresist formulations without prior knowledge of the specific resist or additives chemistry. The rapid approach involves a high resolution measurement of film thickness both before and after hydroxide development. A full kinetics measurement using reflectance Fourier transform infrared (FTIR) spectroscopy combined with modeling may be used to guide predictions for the effects of additives and comparisons between different formulations.

§ Official contribution of the National Institute of Standards and Technology; not subject to copyright in the United States
*vprabhu@nist.gov, tel. (301) 975-3657; fax. (301) 975-3928

Advances in Resist Materials and Processing Technology XXVI, edited by Clifford L. Henderson,
Proc. of SPIE Vol. 7273, 72733U · © 2009 SPIE · CCC code: 0277-786X/09/$18 · doi: 10.1117/12.813555

2. EXPERIMENTAL[#]

2.1 Materials

A commercial EUV photoresist based upon a protected poly(hydroxystyrene) was specially formulated by JSR Micro, Inc. This formulation is a type of environmentally stable chemically amplified positive (ESCAP) polymer. In addition to the pure ESCAP-type polymer without additives, four additional formulations were used that included the ESCAP-type polymer with and without triphenylsulfonium triflate photoacid generator (PAG) and trioctylamine quencher. This led to a total of five formulations in a common spin coating solvent.

2.2 Sample preparation and instrumentation

Model bilayer test structures have been used previously. However, in these cases a different resist polymer pair was used for the top and bottom layers. A technical challenge was to prepare a bilayer with the same resist polymer in both top and bottom layer. Substantial mixing and interdiffusion occurs when trying to perform multiple spin coating on a film of the same material. Floating a polymer film off a substrate onto pure water and transferring to a second polymer film is a routine way to prepare bilayers. However, in this case PAG leaching will change the photoacid distribution. All these problems will make it difficult to make a large uniform area bilayer film suitable for a quantitative analysis.

The sample preparation for our approach was provided in our previous publication.[21] First, a thin film of photoresist polymer without any PAG is spin cast at 2000 rpm (or 209 rad/s) on a clean silicon wafer then post-apply baked (PAB) at 100 °C for 60 s. Then, the top layer photoresist polymer with PAG is spin cast onto a previously-prepared PDMS substrate and stamped onto the PAG-free bottom layer as shown in Figure 1a. After heating for 15 s, the PAG-containing film is transferred to the bottom layer as the PDMS stamp is pealed off. A second PAB is used to remove residual solvent in the top layer. An example of the bilayer prepared on a 76 mm wafer is shown in Figure 1b. The difference in film thickness between the bilayer and single layer may be seen at the wafer edge. The interfacial width between the two layers was determined to be (1 to 2) nm by neutron reflectivity in a poly(methyl methacrylate)/deuterated poly(methyl methacrylate) bilayer system. Although PDMS stamping is used for pattern transfer in microelectronics,[22-24] this is the first time it was used for photoacid diffusion measurements.

Since the PAG is only in the top layer, after deep ultraviolet (DUV) exposure and post-exposure bake (PEB), the generated photoacids diffuse from the top layer to the bottom layer. This approach is an experimental model to the exposed line edge. Due to the sharp initial PAG distribution at the interface (1 to 2 nm), the bilayer corresponds to an image log slope > 600 μm^{-1} and therefore isolates photoacid diffusion effects from lower image log slopes ($\approx$ 90 μm^{-1}) typical for EUV lithography. Such a bilayer structure is also versatile, since the PAG amount or DUV dose may be changed. Further, the PAG or amine quencher may be added in either or both layers generating various diffusion scenarios.

The PEB processed bilayers were developed in 0.26 mol/L tetramethylammonium hydroxide (TMAH) for 60 s followed by 60 s deionized water rinse. The photoacid diffusion length is defined as the development depth into the bottom layer from the initial bilayer interface (Figure 1c). The film thickness after each process step was measured with a J.A. Woollam IR spectroscopic ellipsometer with a standard uncertainty of 1 nm estimated by one standard deviation based upon a calibration with film thickness determined by X-ray reflectivity.

In order to follow the kinetics of the deprotection reaction, FTIR measurements were performed on a customized Nicolet 6700 spectrometer with a J.A. Woollam hot stage with vacuum contact set at the desired PEB temperature. The FTIR spectra were collected upon transfer of the DUV exposed bilayers to the hot stage in reflection mode at 8 cm^{-1} resolution. The time evolution of deprotection (ϕ) was quantified by the absorbance change in a feature band of the resist[21], typically the C–O stretching around 1200 cm^{-1} or 900 cm^{-1}. Silicon wafer substrates were coated with Au to increase the infrared beam reflectivity.

[#] Certain commercial equipment and materials are identified in this paper in order to specify adequately the experimental procedure. In no case does such identification imply recommendations by the National Institute of Standards and Technology nor does it imply that the material or equipment identified is necessarily the best available for this purpose.

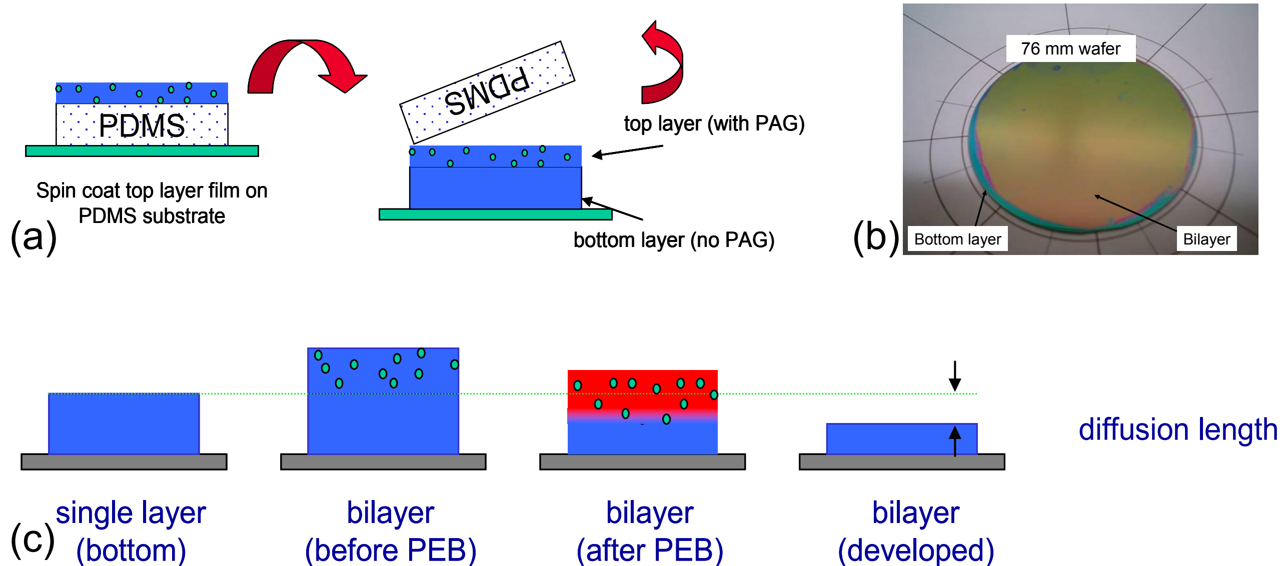

Figure 1. (a) procedure to make bilayers with PDMS stamping technique, (b) a picture of bilayer film sample made with this technique, (c) definition of the diffusion length in the model bilayer.

2.3 Kinetics modeling and methodology

The photoacid diffusion length is dependent upon the resist formulation and process. Each step of the process can be modeled and lead to predictions. The details of the kinetics modeling are provided in a previous publication[21,25] and include the exposure, post-exposure bake and development. In exposure, the photoacid generation is governed by Dill's parameter. In the present case, the sample is exposed to a high dose, so that all the PAG is converted to the photoacid and the photoacid concentration is equal to the initial loading. In the PEB step, the photoacid catalyzed deprotection of the resist, diffusion, trapping, and quenching are described by the following differential equations.

$$\frac{d\phi}{dt} = k_P H(1-\phi) \tag{1}$$

$$\frac{\partial H}{\partial t} = D_H \nabla^2 H - k_T H\phi - k_Q HQ \tag{2}$$

$$\frac{\partial Q}{\partial t} = D_Q \nabla^2 Q - k_Q HQ \tag{3}$$

ϕ, H and Q are the deprotection level, photoacid concentration and quencher concentrations, respectively. The k_P, k_T, and k_Q are the reaction rate constant, trapping rate constant and quenching rate constant, respectively. D_H and D_Q are the diffusion coefficients for the photoacid and quencher, respectively. The parameters may be determined by fitting the experimental data to the three equations. With the parameters known, the deprotection profile can be calculated as a function of PEB time as shown in Figure 2. In the development step, we assume that the resist with deprotection level above a fixed value, called the solubility switch, is removed by developer. Thus, the diffusion length (l_d) is estimated to be the distance between the original bilayer interface and the position at the solubility switch in the deprotection profile as shown by the length between the two vertical lines in Figure 2.

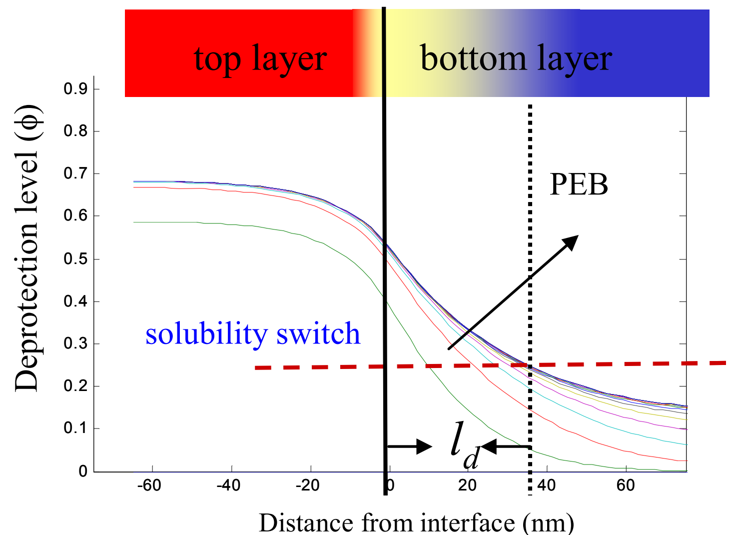

Figure 2. A typical deprotection profile calculated for a bilayer film as a function of increasing PEB time.

3. RESULTS AND DISCUSSION

3.1 Model-free method to characterize the diffusion length: Bilayer contrast curve

An experiment analogous to the traditional contrast curve was completed to estimate the diffusion length for the EUV resist with and without quencher. However, in this case the difference in the thickness between the developed film and the initial bottom layer is the measure of the diffusion length as outlined by Figure 1c. Figure 3 shows the results of this experiment after a PEB at 90 °C for 60 s followed by development in 0.26 mol/L TMAH. The y-axis shows a thickness scale with the origin at the interface of the bilayer films. A positive value indicates that the top layer did not completely dissolve. In contrast, a negative value shows that the reaction propagated into the bottom layer sufficiently to cause a partial development.

Figure 3 shows that the development increases with DUV exposure time, as expected. At low dose, only a few nanometers of the top layer develop, but as the dose increases, the development depth increases until the top layer dissolves completely and the development depth saturates with dose, since all the PAG is converted to photoacid. The average change in film thickness, or l_d, is (36 ± 3) nm, when averaged over the dose-saturated values for the no quencher case. Along these lines the presence of a uniform quencher distribution increases the dose-to-clear for the top layer, as expected. However, the diffusion length l_d was reduced to (14 ± 3) nm, when averaged over the three high dose measurements. While it is known that the quencher reduces the influence of photoacid diffusion, these measurements permit a quantitative comparison without assumption of a kinetic model.

In order to test these laboratory experiments, the same EUV photoresist with quencher was examined by EUV lithography at Intel for various dense half-pitch (HP) sizes (1:1 line/space) as shown in Figure 4. The non-optimized PAB, PEB and development conditions were used to permit a direct comparison to the lab-based experiments. At best focus and 18.5 mJ/cm^2 dose the smallest feature resolved was 36 nm half-pitch. This resolution is very close to the lab determined value of $2\times l_d = (28 \pm 6)$ nm. This comparison demonstrated that the methodology established in the lab can be used to estimate the photoacid diffusion length for a commercial photoresist. This approach is model-free and may provide guidance to evaluate numerous formulations.

A difference between the model line edge and a lithographic line edge is the film loss occurs along different directions, relative to the measured photoacid diffusion length. For the lab sample, the film loss is parallel to model line-edge, while for lithographic features the film loss is perpendicular. Despite the differences, they can be accounted for or estimated for their contribution. The commercial photoresist used in this study, leads to less than 10 % film loss and influences the measurement to ≈ 1 nm.

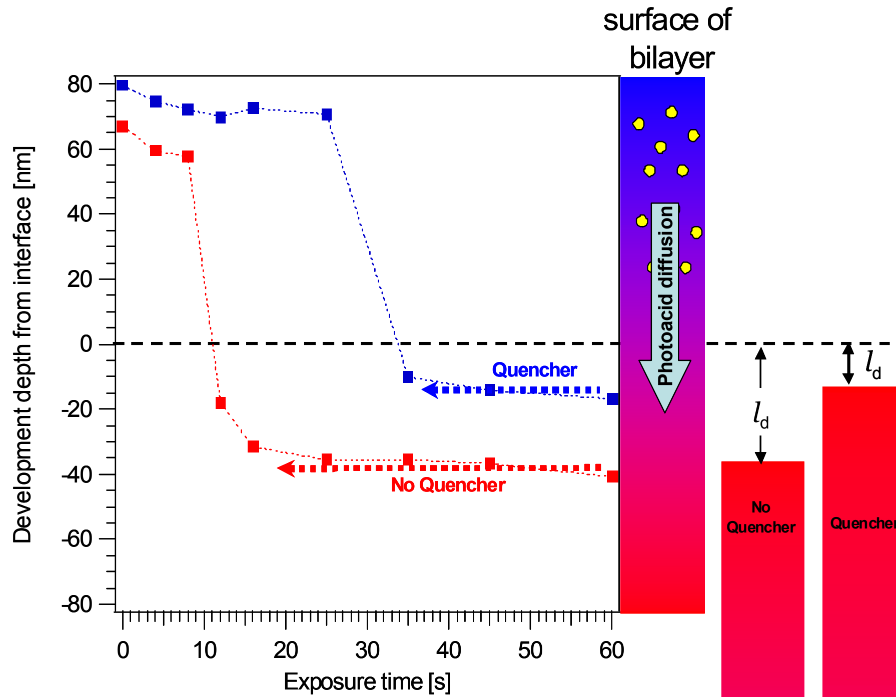

Figure 3. Bilayer contrast curve of development depth versus DUV exposure time (dose) with quencher and without quencher. PAG loading in top layer was 10 % by mass. Lines drawn to guide the reader's eyes. The uncertainty in the measurement is 1 nm.

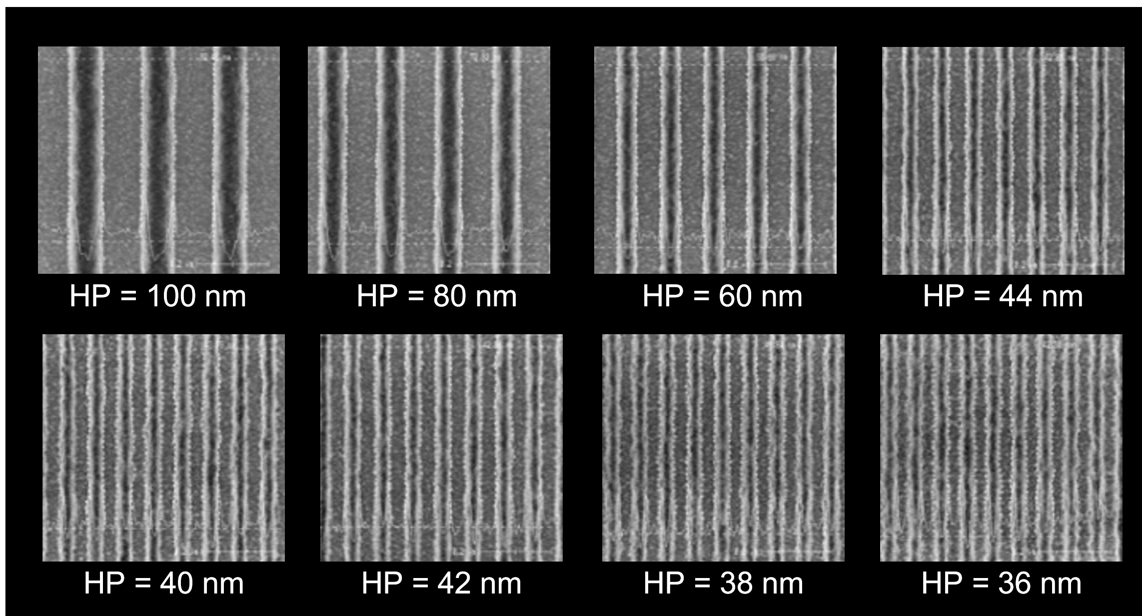

Figure 4. Top-down scanning electron microscope images of dense line-space patterns at best focus and 18.5 mJ/cm^2 dose printed for the EUV resist with quencher at the Intel EUV photolithography facility. The half-pitch (HP) is provided beneath each image. The resist, PAB, PEB and development conditions are the same as in Figure 3.

3.2 Prediction of the photoacid diffusion length

In a commercial photoresist, if the photoacid diffusion length is too large, then multiple formulations or process conditions must be screened. This is a time-consuming and costly process. The proposed bilayer methodology provides

a convenient and direct method to estimate l_d and make comparisons. The modeling strategy described previously was used to gain further insight into the photoacid diffusion length and effect of quenchers.

Four types of samples were prepared with the amine quencher located in different layers of the bilayer films as shown in Figure 5. All samples were processed identically with 150 mJ/cm^2 248 nm DUV exposure, PEB of 90 °C for 900 s, and development in 0.26 mol/L TMAH for 60s followed by 60 s DI water rinse. The FTIR kinetics data (Figure 6a) were collected for each of sample and fit to the kinetics model. The resulting kinetics parameters are provided in Table 1. With these parameters, the PEB time-dependent deprotection profile was calculated for the different bilayer conditions as shown in Figure 6b. The intersection of these profiles with a common solubility switch leads to a predicted diffusion length. In this case the solubility switch is a parameter. Table 2 shows the comparison of measured and predicted photoacid diffusion length. The photoacid diffusion length is largest without quencher (sample #1), as expected, and a

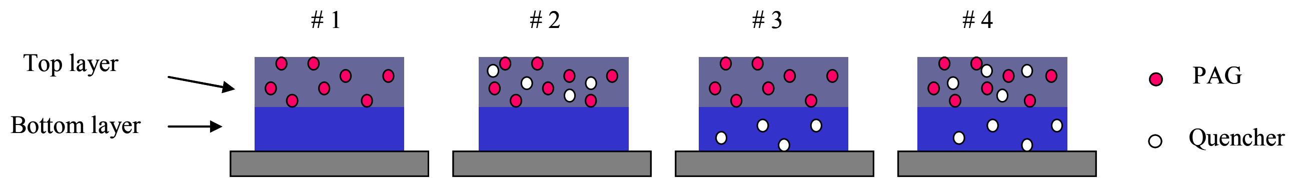

Figure 5. Quencher layout for four bilayer samples. The PAG loading at top layer was 2 % by mass and the quencher loading was 60 % by mole relative to the PAG concentration.

Table 1. The fitted kinetics parameters for the JSR EUV commercial photoresist at PEB of 90 °C.

k_P (nm^3/s)	k_T (s^{-1})	D_H (nm^2/s)	k_Q (nm^3/s)	D_Q (nm^2/s)
1.6 ± 0.1*	0.026 ± 0.002	4.2 ± 1.3	1.6 ± 1.0	7.3 ± 3.0

* Uncertainty is estimated by one standard deviation of an average of three measurements

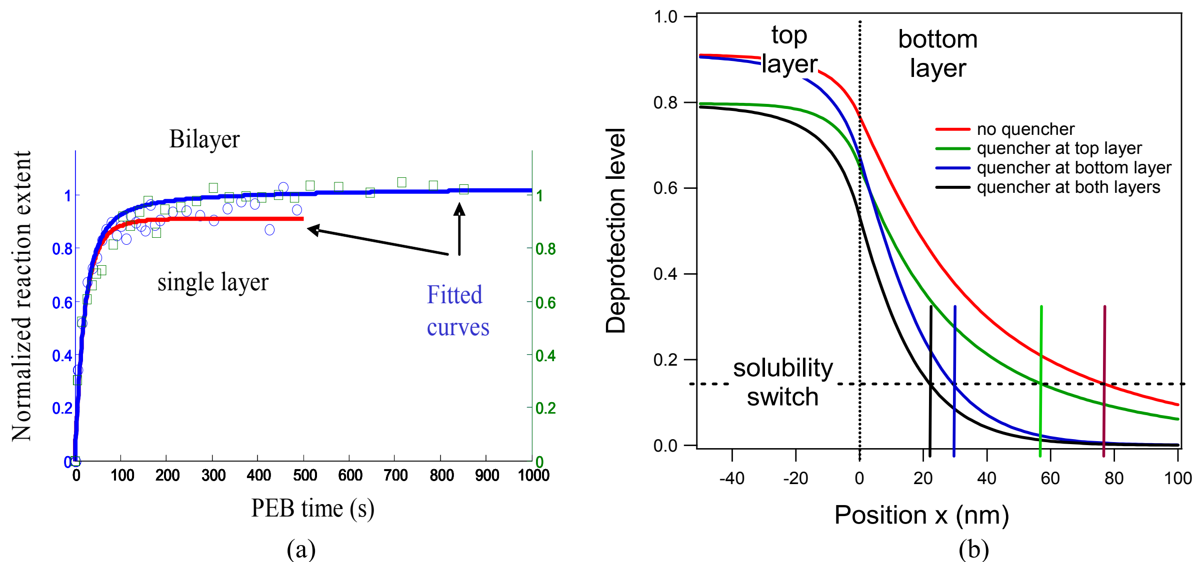

Figure 6. (a) Time evolution of reaction extent for a single layer sample and bilayer sample containing the same amount of PAG. The reaction extent is normalized to top layer film and therefore may be greater than one. (b) Calculated deprotection profiles based upon the kinetics parameters in Table 1. The solubility switch of 0.14 closely matches the predicted to measured thickness.

minimum for uniform quencher distribution (sample #4). However, comparing sample # 2 and sample # 3, the quencher in the bottom layer is more efficient in reducing l_d. This case mimics the situation of a photodegradable base that is deactivated upon DUV exposure.[26] In the above cases, Table 2 also shows that the predicted and the measured l_d agree with each other very well with a single solubility switch. Therefore, quantitative comparisons can be made among different experimental conditions in a self-consistent manner. Further, if a chosen theoretical model is applied, either through our approach or other methods, further insight is gained that can lead to diffusion length predictions, thus paving a way for rapid screening of process conditions. The difference in the diffusion length without and with uniform quencher in section 3.1 and this section is due to the difference in PEB time.

Table 2. Measured and predicted photoacid diffusion length for JSR EUV photoresist at PEB of 90 °C

Sample , quencher layout in Scheme III	# 1 No Quencher	# 2 Quencher in top layer	# 3 Quencher in bottom layer	# 4 Quencher in both layers
Diffusion length: Measured[1] [nm]	76	56	36	23
Predicted[2] [nm]	79	59	30	23
Calculated gradient at solubility switch [1/nm]]	2.5	3.0	8.8	8.9

[1] Model-independent approach through film thickness change upon development. The uncertainty in the diffusion length is ≈ 2 nm, estimated by one standard deviation.
[2] Based upon calculated deprotection profiles and development at common solubility switch.

3.3 Implications for resist design

The kinetics parameters reflect the resist material properties such as PAG size and acidity, resist polarity and glass transition, therefore guidelines that correlate materials properties with the kinetic parameters to achieve shorter diffusion length would be useful. A diffusion length can be predicted from the known parameters as shown in the previous section. Inversely, one may fix the photoacid diffusion length and determine the set of kinetic parameters that meet this constraint. Therefore, the problem may be reduced to finding a combination of k_P, k_T and D (assuming no quencher) that leads to a fixed l_d.

Based on the kinetics model, the combinations of kinetics parameters required to meet a target diffusion length of 16 nm was calculated. Using the relationship determined earlier this would correspond to a ≈ 32 nm half-pitch resist resolution. The process condition used in the calculation matches our previous experimental results.[21] Specifically, Q = 0, H_0 = 0.065 nm^{-3} (≈ 5 % by mass PAG), PEB t = 60 s, and SW = 0.2. For each pair of fixed k_P and D, the value of k_T is changed until the diffusion length equals 16 nm at the solubility switch. Through this iterative procedure five values of D were examined and shown by the set of symbols in Figure 7a. Each family of data points for a fixed D represent the criteria of l_d = 16 nm. Above each family are conditions where l_d < 16 nm and below each family l_d > 16 nm. For the D = 16 nm^2/s case, shown as (∗), above the line fit to the data would be parameters that lead to a diffusion length less than 16 nm.

These calculation results of Figure 7a were fit with an empirical relationships, $k_T = 0.06\sqrt{D}\ln\frac{k_P}{k_P^0}$ and $k_P^0 = 0.3e^{2.3/D}$, shown as the solid lines and replotted in Figure 7b as a curved surface in the parameter space of k_P, k_T and D. In this representation, the parameter space below the surface represents the set of kinetics parameters such that l_d > 16 nm. In such a case, either the k_P and D are too large, or the k_T is too small. Reducing k_P and D is not favorable to EUV photolithography because it implies a decrease in the photosensitivity. Therefore, the only choice left is to enhance the phenomenological trapping constant, k_T, a quantity reflecting the interaction strength between the photoacid and the polar groups in the deprotection products.

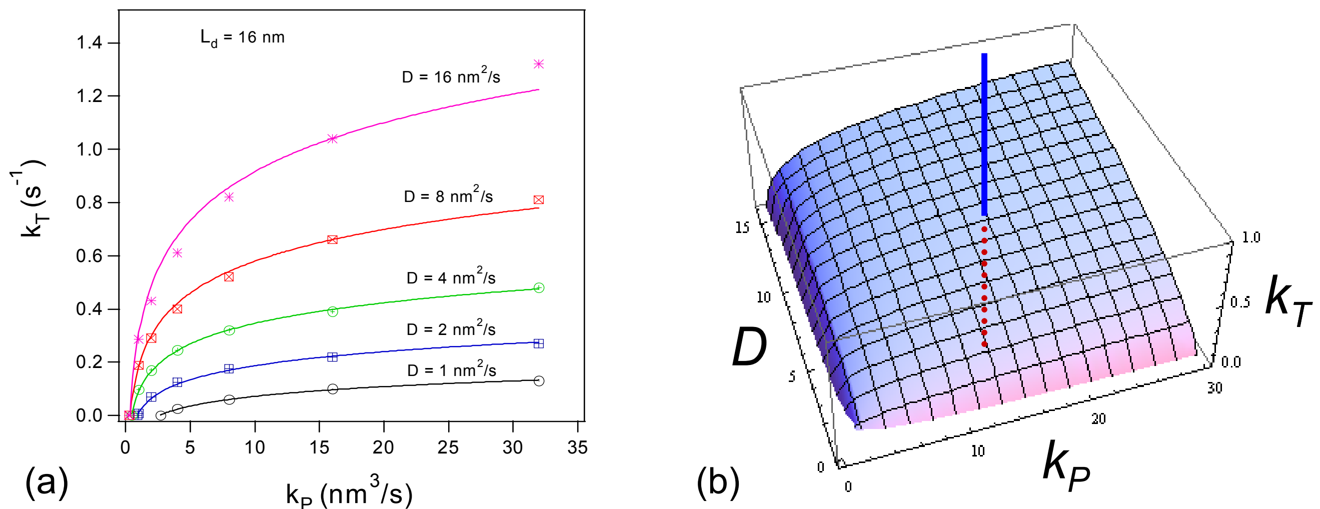

Figure 7. (a) Combination of parameters that produce a maximum photoacid diffusion length of 16 nm. (b) Threshold surface for 16 nm diffusion length based on empirical relations fit to the data in (a).

Adding quencher is the most common way to reduce the adverse affects of photoacid diffusion. However, is there any advantage for enhancing photoacid trapping over adding quencher? We know that both quenching and trapping mechanisms cause acid loss because of the separate terms $-k_Q HQ$ and $-k_T H\phi$ in Equation (2). In the quencher case, the quencher deactivates the photoacid through neutralization, while a trapping agent like a carboxylic group or phenolic group deactivates the photoacid by reducing or eliminating photoacid mobility through hydrogen-bonding interactions. The apparent reaction constant is relatively smaller for trapping than quenching as shown in Table 1.

An important difference is that the quenching and trapping mechanisms cause photoacid loss at different stages of the reaction time (conversion). Since the quencher concentration is initially a maximum, the acid loss is also maximum at the initial PEB times, while the trapping effect become significant only at the later stages because the deprotection level ϕ is initially very small. This difference generates some interesting consequences on LER and CD control. Figure 8 are simulated deprotection profiles produced by either quenching or trapping. The trapping constant is made greater than experimentally determined to generate a profile similar to the quenching case at high dose. It can be seen that at high dose (Figure 8a) both trapping and quenching lead to a small diffusion length and high deprotection gradient at the solubility switch that implies low LER.[27] However at low dose (Figure 8b), the quencher reduces the photoacid concentration leading to a lower deprotection level in the exposed area, resulting in a rough line edge as seen by the local deprotection slope at the solubility switch. On the contrary, the trapping mechanism avoids this problem because the photoacid is lost at a later stage of reaction. Therefore, the deprotection level is high enough in the exposed region leading to a sharp gradient at solubility switch, hence low LER. Therefore using trapping could be a better choice than quenching in this situation.

For many EUV or 193 nm photoresists, the trapping strength is not sufficient to achieve a 16 nm diffusion length, therefore a quencher is added. Currently, resists are chosen with functional groups that weakly interact with the photoacid at the protected state, but strongly interact in the deprotected form. Such examples are protected carboxylic, phenolic, or hexafluoroisopropanol groups already used in DUV and EUV photoresists. If photoresists can be prepared to avoid an early loss of photoacid, or photosensitivity, but deactivate the photoacid once the reaction is reached to a satisfactory level then one may break the trade-off in sensitivity, dose, and resolution.

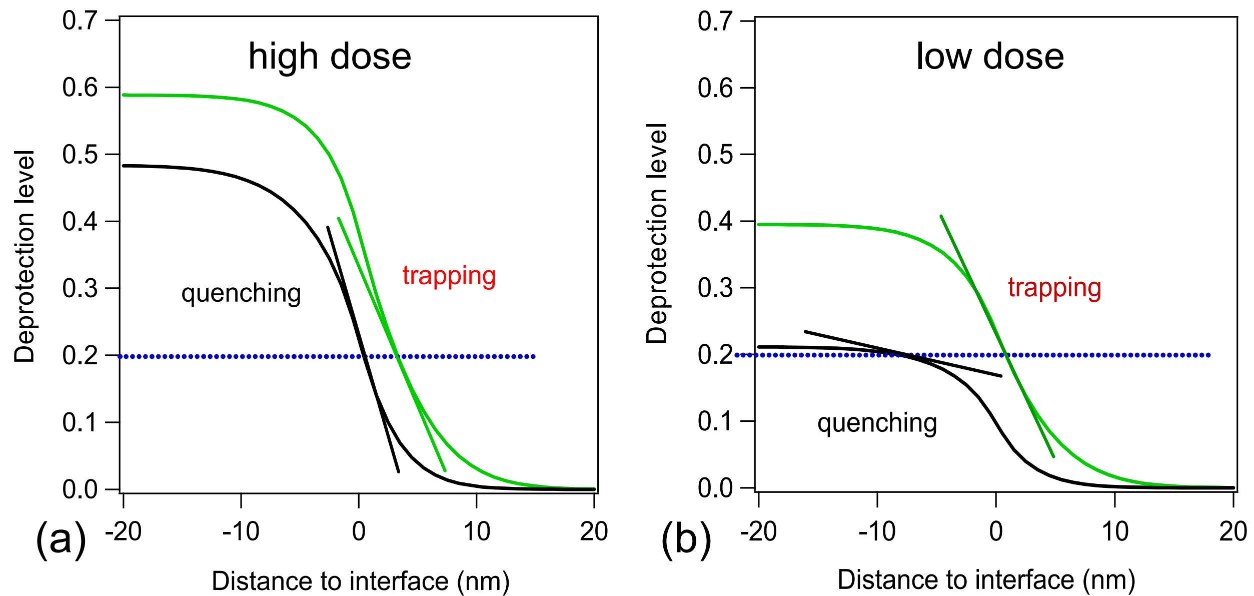

Figure 8. Simulated deprotection profiles produced by either trapping or quenching processes. (a) high dose; (b) low dose. Notice that a trapping process introduces a higher deprotection slope at the solubility switch, necessary for low LER.

4. CONCLUSIONS

A bilayer stack technique was used to characterize the photoacid diffusion length through a combination of film thickness and FTIR measurements. Using a commercial EUV photoresist, the photoacid diffusion length measurement correlated with EUV lithographic results such that $2\times\ l_d \approx$ minimum CD printed. These diffusion length measurements were verified by applying a kinetics model that reproduced the deprotection profiles under four different amine-quencher loading conditions. Further, the kinetics model was inverted to formulate a criteria for the kinetics parameters that must result in a fixed photoacid diffusion length. Based on this approach, the photoacid trapping process would be beneficial to design into photoresist formulation because it does not reduce resist sensitivity, but controls the latent image profile and CD at low dose. This trapping process is mechanistically different from amine quenchers through the first order the scaling of trapping rate with the photoacid and deprotection product concentration.

5. ACKNOWLEDGEMENTS

This work was supported by a cooperative research and development agreement between the Intel Corporation and NIST (NIST CRADA 1893) and the NIST Office of Microelectronics Programs. We acknowledge Michael Leeson, Steve Putna, Christof Krautschik, George Thompson from Intel, and Chris Soles from NIST for their support and Yoshi Hishiro of JSR Micro for the EUV photoresist formulations used in this study.

REFERENCES

[1] Bristol, R. L., "The tri-lateral challenge of resolution, photospeed, and LER: scaling below 50nm?", SPIE, 6519, 65190W-651911 (2007).

[2] Gallatin, G. M., Naulleau, P., Niakoula, D. and others, "Resolution, LER, and sensitivity limitations of photoresists", SPIE, 6921, 69211E-11 (2008).

[3] Van Steenwinckel, D., Gronheid, R., Lammers, J. H. and others, "A novel method for characterizing resist performance", SPIE, 6519, 65190V-651911 (2007).

[4] Wu, B. and Kumar, A.,"Extreme ultraviolet lithography: A review," J.Vac.Sci.Technol.B., 25(6), 1743 (2007).

[5] Ito, H.,"Chemical amplification resists for microlithography," Adv.Polym Sci., 172, 37 (2005).

[6] Ito, H.,"Rise of chemical amplification resists from laboratory curiosity to paradigm enabling Moore's law," Proceedings of SPIE, 6923, 692302_1-692302_15 (2008).

[7] Van Steenwinckel, D., Lammers, J. H., Leunissen, L. H. A., and Kwinten, J. A. J. M.,"Lithographic Importance of Acid Diffusion in Chemically Amplified Resists," Proceedings of SPIE, 5753, 269 (2005).

[8] Schnattinger, T. and Erdmann, A.,"A comprehensive resist model for the prediction of line-edge-roughness material and process dependencies in optical lithography," Proceedings of SPIE, 6923, 69230R_1-69230R_12 (2008).

[9] O'Connor, N. A., Berro, A. J., Lancaster, J. R. et al.,"Toward the Design of a Sequential Two Photon Photoacid Generator for Double Exposure Photolithography," Chemistry of Materials, 20(24), 7374 (2008).

[10] Byers, J., Lee, S., Jeri, K. et al.,"Double exposure materials: Simulation study of feasibility," Journal of Photopolymer Science and Technology, 20(5), 707 (2007).

[11] De Silva, A., Felix, N. M., and Ober, C. K.,"Molecular glass resists as high-resolution patterning materials," Advanced Materials, 20(17), 3355 (2008).

[12] Felix, N. M., De Silva, A., and Ober, C. K.,"Calix[4]resorcinarene derivatives as high-resolution resist materials for Supercritical CO2 processing," Advanced Materials, 20(7), 1303-+ (2008).

[13] De Silva, A., Lee, J. K., Andre, X. et al.,"Study of the structure-properties relationship of phenolic molecular glass resists for next generation photolithography," Chemistry of Materials, 20(4), 1606 (2008).

[14] Shirota, Y.,"Photo- and electroactive amorphous molecular materials—molecular design, syntheses, reactions, properties, and applications," J.Mater.Chem., 15, 75 (2005).

[15] Bratton, D., Yang, D., Dai, J., and Ober, C.,"Review: Recent progress in high resolution lithography," Polym.Adv.Technol., 17, 94 (2006).

[16] Fukushima, Y., Watanabe, T., Ohnishi, R. et al.,"Optimization of Photoacid Generator in Photoacid Generation-Bonded Resist," Japanese Journal of Applied Physics, 47(8), 6293 (2008).

[17] Lawson, R. A., Lee, C. T., Yueh, W., Tolbert, L., and Henderson, C. L., Single molecule chemically amplified resists based on ionic and non-ionic PAGs, SPIE, 6923, 69230K-692310 (2008).

[18] Wang, M. X., Gonsalves, K. E., Rabinovich, M., Yueh, W., and Roberts, J. M.,"Novel anionic photoacid generators (PAGs) and corresponding PAG bound polymers for sub-50 nm EUV lithography," Journal of Materials Chemistry, 17(17), 1699 (2007).

[19] Wang, M. X., Lee, C. T., Henderson, C. L. et al.,"Incorporation of ionic photoacid generator (PAG) and base quencher into the resist polymer main chain for sub-50 nm resolution patterning," Journal of Materials Chemistry, 18(23), 2704 (2008).

[20] Wu, H. P. and Gonsalves, K. E.,"Preparation of a photoacid generating monomer and its application in lithography," Advanced Functional Materials, 11(4), 271 (2001).

[21] Kang, S., Lavery, K. A., Choi, K. W. et al.,"A comparison of the reaction-diffusion kinetics between model-EUV polymer and molecular-glass photoresists," Proceedings of SPIE, 6923, 692317_1-692317_12 (2008).

[22] Schmid, H. and Michel, B.,"Siloxane Polymers for High-Resolution, High-Accuracy Soft Lithography," Macromolecules, 33(8), 3042 (2000).

[23] Odom, T. W., Love, J. C., Wolfe, D. B., Paul, K. E., and Whitesides, G. M.,"Improved Pattern Transfer in Soft Lithography Using Composite Stamps," Langmuir, 18, 5314 (2002).

[24] Park, D. S., Kim, K., Pillans, B., and Lee, J. B.,"Polydimethylsiloxane-based pattern transfer process for the post-IC integration of MEMS onto CMOS chips," J.Micromech.Microeng., 14, 335 (2004).

[25] Kang, S., Wu, W. L., Prabhu, V. M. et al.,"Evaluation of the 3D compositional heterogeneity effect on line-edge-roughness," Proceedings of SPIE, 6519, 65193V_1-65193V_10 (2007).

[26] Vogt, B. D., Kang, S. H., Prabhu, V. M. et al.,"Influence of base additives on the reaction-diffusion front of model chemically amplified photoresists," Journal of Vacuum Science & Technology B, 25(1), 175 (2007).

[27] Pawloski, A. R., Acheta, A., Levinson, H. J. et al.,"Line edge roughness and intrinsic bias for two methacrylate polymer resist systems," J.Microlith., Microfab., Microsyst., 5(2), 023001_1-023001_16 (2006).